HOVER PERFORMANCE ASSESSMENT OF 3 METER RADIUS ROTOR ON WHIRL TOWER

Alper EZERTAS, Arda YUCEKAYALI, Yüksel ORTAKAYA
Turkish Aerospace Industries, Inc.
Ankara Turkey
aezertas@tai.com.tr, ayucekayali@tai.com.tr, yortakaya@tai.com.tr

Abstract

Hover aerodynamic performance characterization of the indigenously designed 3 meter radius main rotor, which will be installed on rotary wing UAVs, is performed by analyses and tests. Manufactured full scale prototype is tested on the in-house designed whirl tower which is instrumented to enable measurement of thrust, torque, blade aeroelastic response, wake characteristics and aeroacoustic noise. The effects of the collective setting variation on the sectional and cumulative performance characteristics of the rotor are investigated. Quantitative and qualitative downwash rotor wake measurements are applied by an array of fast response 5-hole probes and visualization of entrained smoke in the flow field, respectively. Aerodynamic analyses are conducted by using RANS CFD solvers and comprehensive analyses tools. Analysis tools are validated with experimental data available in literature before they are utilized in the evaluation of performance and flowfield of the designed rotor. Comparing the collected data from whirl tower tests and analysis outputs resulting aeromechanic characteristics of the designed rotor is assessed. Following the compliance of the required aeromechanic performance of the designed rotor by the analysis and tests, the rotor is installed on the built unmanned rotorcraft prototype. Test and measurement capability developed on the whirl tower will be extended by flight tests of the designed indigenous platform.

1 INTRODUCTION

The decision made by designer on the radial distribution of blade-chord, airfoil section and twist has a direct impact on the hover performance of the rotor by influencing the induced flow field. Hence reliable analysis tools are required to be able to reflect the effect of each design parameter properly in the calculations carried out in the design phase. The uncertainties in the analysis tools and design concept itself shall be eliminated by employing dedicated tests on proper setups before finalizing the design phase. Whirl tower test systems are widely used setups which are capable of measuring the hover performance of the new designs conveniently [1,2,3]. Moreover those setups can also be used to examine the structural integrity and dynamic balance of the rotor system and power transmission of active systems in rotating frame can be demonstrated.

TAI has been investing the development of an infrastructure which will enable required analyses and tests through the design phase of new rotorcraft platforms. Among the contractual projects experimental programs for development of light weight unmanned rotorcraft has also been carried out in last two years. This study focuses on outlining the initial efforts applied for aeromechanical analysis and tests of 3 meter radius rotor designed and manufactured in TAI.

The aeromechanic design of an indigenous 3 meter radius rotor, which will be installed on rotary wing UAV, is completed by using engineering tools that have been validated through previous research and contractual programs. Full scale prototype of the designed rotor is manufactured and mounted on the whirl tower tests facility which was also designed indigenously. The hover performance of the prototype is tested with various measurements from different disciplines and collected results are compared with the predictions of analyses applied through the design phase. The main motivations behind the study was to be able to acquire full scale rotor whirl tower testing capability, validating the hover performance of the designed rotor system and validating the computational tools employed during the design phase.

The hover tests applied for Caradonna-Tungs's experimental model rotor and full scale rotor of the BO105 helicopter rotor are chosen as validation tests cases and evaluated results are presented in following chapters after giving brief information about the analysis tools that are used. Validation related subchapters are followed by the presentation of the analysis and tests results attained for the designed rotor system. The study is finalized with the conclusion made on the compliance of the measured characteristics of the designed rotor with the required performance.

2 AERODYNAMIC ANALYSIS AND VALIDATION OF THE TOOLS

The aerodynamic characteristics of the designed rotor are evaluated using both comprehensive and CFD analysis tools in design stage. Validation studies were carried out for each analysis tool for performance assessment of hovering rotor problem with available data in literature. Using the validated tools the performance characteristics of the designed rotor is outlined and the predicted hover characteristics are compared with the test results measured from the whirl tower.

2.1 Blade Element Theory Based Analysis

The low fidelity aerodynamic modeling of the rotor is performed by using the commercial comprehensive analysis tool, FlightLab. Airloads are predicted with a quasi-unsteady approach. Various inflow and wake models at different complexities are used to calculate

Presented at the 39th European Rotorcraft Forum, Moscow, Russia, September 3-6, 2013.

induced velocity distribution over the rotor disc. Rotor total thrust, torque and power values are evaluated with the inflow, effective angle of attack and aerodynamic load distributions over the blade span. Additionally, an in-house developed isolated rotor analysis tool, xBEM, is used to mathematically model the rotor and predict the total thrust generation and power requirement. xBEM uses prescribed wake geometry and vortex-wake method to determine aerodynamic force and moment distributions over the rotor disc. Integration of the aerodynamic load distributions results in total force and moments generated by the rotor.

2.2 CFD Analysis

The CFD analyses are carried out by using commercial tool ANSYS Fluent. The hover analyses are performed by solving the moving reference frame form of RANS equations. The flow field is assumed to be fully turbulent and one equation Spalart Allmaras turbulence model with curvature correction is utilized in the analyses. The flow equations are discretized by pressure based approach where the constraint of continuity of the velocity field is achieved by solving a pressure equation[4]. The resulting momentum and pressure-based continuity equations are solved together with a fully implicit coupling[5]. The Rhie-Chow based method is followed for discretization of the pressure based continuity equation. The MUSCL scheme is utilized for spatial discretization[6]. The pseudo transient under relaxation method is utilized to speed up the convergence rate of the steady solutions.

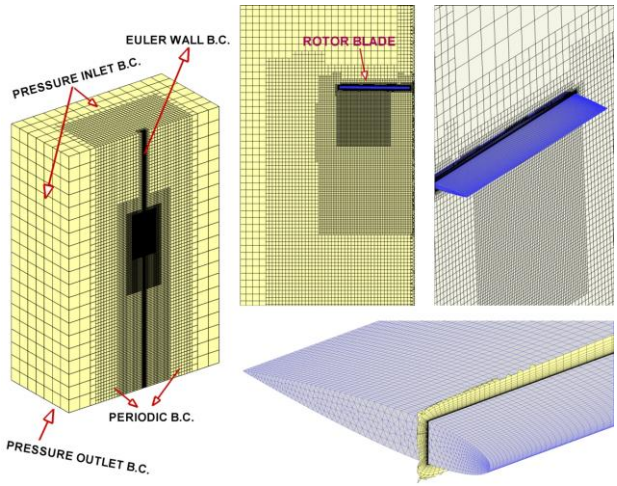

Figure 1 Mesh topology applied in the hovering rotor CFD analyses

The periodic boundary conditions, which enable reduction of the flow domain to be discretized, are applied to lessen the computational burden. The near field mesh around rotor blade is generated with body conforming prismatic cells composed of 30 layers in total and heights of the cells in the first layer is constrained to satisfy y+ values lower than 1 on the blade surface. Far field mesh is generated by the cartesian grid type hexcore topology using the grid generation software Tgrid. In the analyses 7 to 9 level of mesh refinement from outer boundaries to the near mesh surrounding the blade surface is applied by hanging nodes to enhance the vortical wake resolution. The region with finest mesh resolution is extended from rotor to the downwash region by one rotor radius distance. The mesh region with succeeding refinement level extends to 3 rotor radius distance below the rotor. The mesh cell size is gradually increased below 10 rotor radius distance in the downwash region. The farfield boundaries are located away from the rotor center by 20 rotor radius distance in the upwind and sideway directions. The boundary of the domain below the rotor is located 40 rotor radius distance away. Isoclips taken at constant azimuth from typical flow domain is presented in Figure 1 to outline an example mesh topology utilized in the hover analysis. The number of mesh elements in the analyzed domain varies between one million to five million depending on the level of refinements and cell edge length

The followed CFD method with steady state solutions does not depend on relatively large computational resource. Single RANS analysis of a hovering rotor was able to be completed in 10 to 20 hours on single workstation computer which has 16GB of memory and four cores on its processor that has 3GHz clock speed.

2.3 Validation with Carradonna Tung Rotor

Caradonna and Tung carried-out experiments for hovering model helicopter rotor which has 1.143m radius[7]. The blade pressure is measured at 5 different radial stations by 60 pressure tubes and tip vortex position along the wake of the hovering rotor is extracted by traversing a hotwire in the flow field. The results of the test campaign was widely used through the literature as reference for validation of numerical analysis tools developed for rotary wing aerodynamics problems [8,9,10].

The reliability of the flow field generated for hovering rotor by using current CFD methodology is examined against Caradonna Tung test results. Basically two different meshes were utilized for the analyses. The first mesh was constructed with finest cell edge size equal to 0.06 chord length whereas in the second mesh the edge length on the finest cells equals to 0.12c. 4.2 million cells are utilized for the generation of the finer mesh while the second mesh involves 1.6 million elements.

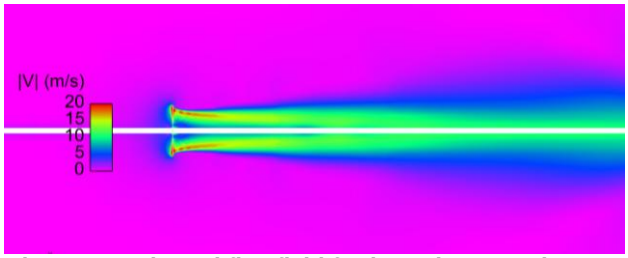

Figure 2 Evaluated flowfield for hovering rotor by CFD

The appropriateness of the applied boundary conditions and mesh resolution for capturing the hovering rotor flowfield is assessed by observing the calculated velocity fields. Figure 2 presents the computed velocity magnitude contours on plane extracted from the flowfield at constant azimuth ($\Psi = 0°$). Evaluating the flow field depicted in Figure 2 qualitatively it can be stated that, excitation of the still air by rotor and resulting flowfleld is captured properly by the analyses. The generated downwash extends to the farfield boundary located 40 rotor radius below the rotor center where pressure outlet type boundary condition is applied. The variation of the

evaluated flowfield is smooth and no anomaly in pressure and velocity contour plots were observed near to boundaries.

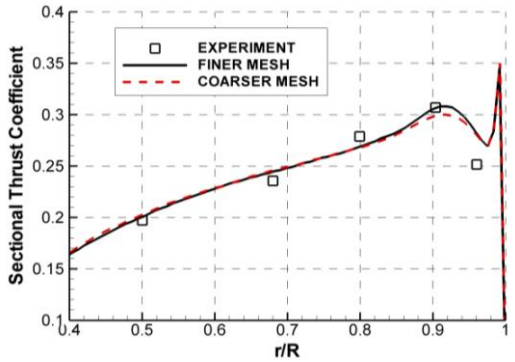

Figure 3 Sectional thrust coefficient distribution on Caradonna Tung rotor blade (Ω=1250 rpm, θ = 8°)

The sectional thrust coefficient variation evaluated on Caradonna Tung blade for 8 degrees of collective setting is compared with the experimental results in Figure 3 Considering the mesh size and computational effort spent the consistency of the CFD results with experimental data is satisfactory and promising for further analyses. The refinement of the cell edge size on finest mesh level from 0.12c to 0.06c did not introduce a notable enhancement on the sectional thrusts results.

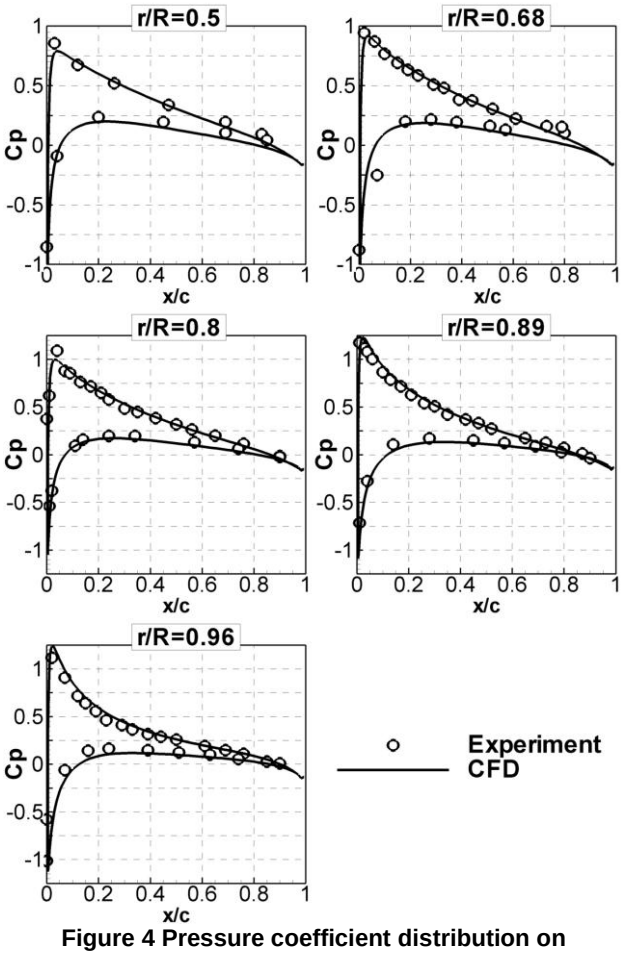

Figure 4 Pressure coefficient distribution on Caradonna Tung rotor blade (Ω=1250 rpm, θ = 8°)

The proficiency level in prediction capability of surface pressure variation is crucial in design phase of a rotor blade since it is one of the major components of the airloads. Moreover the surface pressure variation over the blade surface is a crucial aeroacoustic noise source. Carradonna Tung tests outlined valuable validation opportunities by presenting experimental surface pressure data of hovering rotor at different collective settings and tip speeds. Figure 4 presents comparison of the experimental surface pressure coefficient with results obtained by CFD solutions over mesh composing 1.6 million cells. Comparison of the results exhibits good consistency.

The dependence of rotor tip vorticity capturing on mesh resolution is investigated by comparing post processed CFD results evaluated by coarse and finer mesh. Figure 5 presents the iso-surfaces generated for second invariant of velocity gradient, q criterion for 8 degrees of collective and 1250 rpm rotational speed condition. Depicted tip vorticity structures showed that mesh resolution affected the tip vorticity preservation notably. While tip vorticity can be identified through 2 rotor revolutions with coarse mesh it is apparent for almost 4 revolutions when finer mesh is used in the analysis.

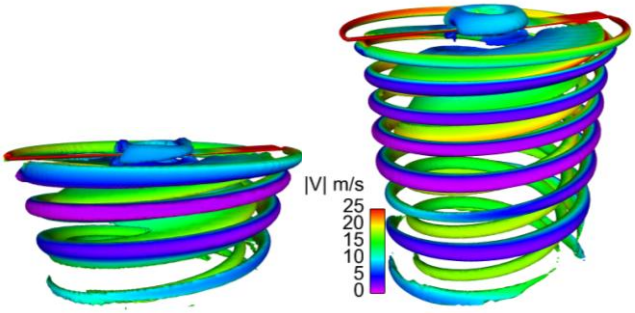

a) Coarse mesh b) Finer mesh

Figure 5 Iso-surfaces of *q* = 1.0 (normalized by tip speed and chord) colored by velocity magnitude.

The evaluated radial contraction and the axial convection of tip vortex trajectory by using the finer mesh is compared with the experimental data in Figure 6. Results show that tip vortex position is captured successfully with the followed CFD methodology.

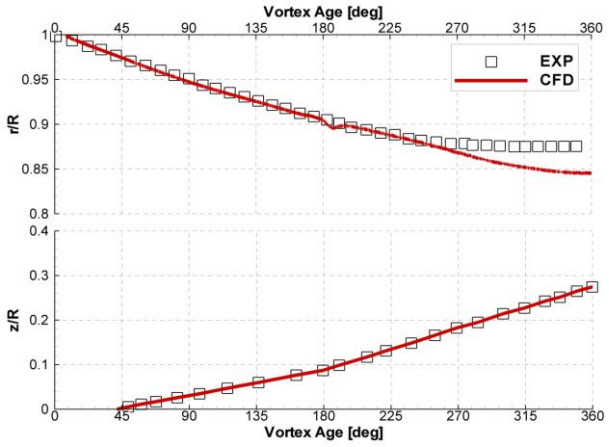

Figure 6 Position of Tip vortex through the downwash of Caradonna Tung rotor (Ω=1250 rpm, θ = 8°)

2.4 Validation with BO105 Rotor

The full scale hingeless rotor of the BO105 helicopter was tested in the NASA Ames 40- by 80-Foot Wind Tunnel by Peterson et.al [11]. Experimental data was collected for performance, loads and aeroelastic stability of the rotor throughout the tests. The test data published [12] for hover performance of the rotor at varying collective settings is used as reference for assessing the capability of the aforementioned CFD methodology, developed mathematic model and commercial tool Flightlab for thrust generation and power requirement prediction. Figure 7 presents the comparison of the evaluated hover performance results of BO105 rotor with the test data. All utilized analysis tools yielded results at pleasing accuracy for varying operation conditions at hover.

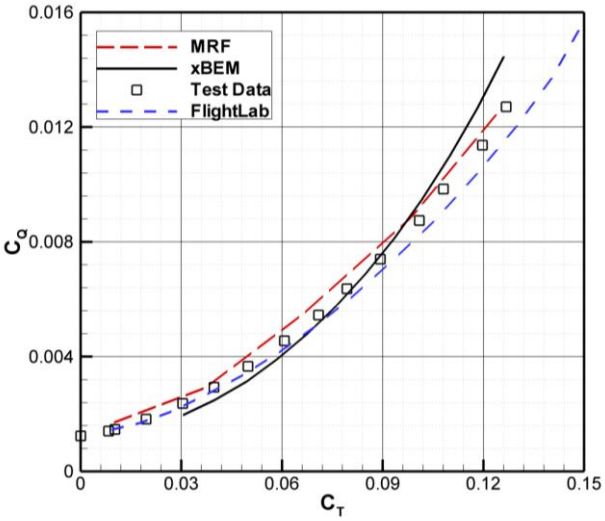

Figure 7 Validation of analysis tools for performance prediction of hovering BO105 rotor

3 XSAR_V11 ROTOR DESIGN

Rotor and hub system tested and analyzed in this study is a baseline prototype designed and manufactured specifically for the family of rotary wing UAV designs of TAI. The aeromechanic design of the blade is carried out with validated tools. The specifications of the tested prototype are presented in Table 1. The tested baseline rotor has straight blade tip shape. In near future two different blade tip shapes with varying taper, sweep, dihedral and chord length characteristics will be tested.

Table 1 Specifications of the tested rotor prototype

Blade Span	3 m
Nominal rotational speed	540 rpm
Tip Mach # Interval	0.5-0.8
Twist Angle (linear)	16°
Cone Angle	2°
Root-Cut Out	10%

The manufactured full scale prototype is tested on whirl tower more than 100 hours for aeromechanic and aeroelastic measurements until the second half of 2013. The blades are also installed on the experimental unmanned rotorcraft, HC1, manufactured in TAI which has 400 kg of maximum takeoff weight. One of the manufactured blades is instrumented with strain gauges to collect elastic deformation information. Same flight test instrumentation box is able to be mounted on both the whirl tower and unmanned rotorcraft platform, hence it is possible to measure blade aeroleastic response during both rig and flight tests. Part of the ground tests of HC1 platform was carried out in first half of 2013 and the first flight test is scheduled in the third quarter of 2013. Figure 8 presents a photo which shows the ground tested HC1 platform equipped with the designed rotor in front of the whirl tower facility.

Figure 8 Designed rotor blade is installed on HC1 unmanned rotorcraft (400 kg MTOW)

4 WHIRL TOWER TESTS

The TAI Whirl Tower test system, TWT is equipped with a 630kW electric motor. The test facility enables testing of rotors that have blade radius up to 8 meters. The test facility and baseline rotor blade with straight tip are depicted in Figure 9 by photographs taken from test facility. Different hub types can be tested with the interchangeable rotor head. Whirl Tower test setup is equipped with adequate instrumentation to measure the aerodynamic performance and downwash velocity, visualize the wake and evaluate acoustic signature of the tested rotor system.

Figure 9 TAI Whirl Tower (TWT)

The primary purpose of the hover tests performed at TWT is to characterize the hover performance of the designed rotor for varying blade pitch setting and rotational speed in terms of aeromechanics aspects. Prior to flight tests, it is crucial to ensure the integrity of swash plate, hub, hub links and blade system with each other. Additionally, testing a full scale prototype serves to investigate geometric, dynamic, aerodynamic scaling and fabrication detail effects on rotor performance.

4.1 Thrust& Power measurement

Whirl Tower tests are carried out for various rotational speeds up to 600 rpm and collective angle settings up to 16 degrees. Thrust and torque values are measured by load cell installed on rotor shaft below the hub. Hover

performance prediction of the utilized aerodynamic analyses tools are compared with the applied measurements. These comparisons enable assessing the consistency of the resulting performance of the manufactured rotor with the intended performance from design which was defined by analyses. Figure 10 and Figure 11 presents the comparison of analysis and the measurements for the thrust generation and power requirement characteristics of the designed rotor respectively. The results presented in these two figures are predicted and measured for rotor operating at 540 rpm rotational speed. Results show that analysis tools predicted the thrust values with a satisfactory accuracy. Predicted and measured power requirement results show also good agreement although the predictions with developed tool xBEM resulted in a bit higher power values for higher collectives.

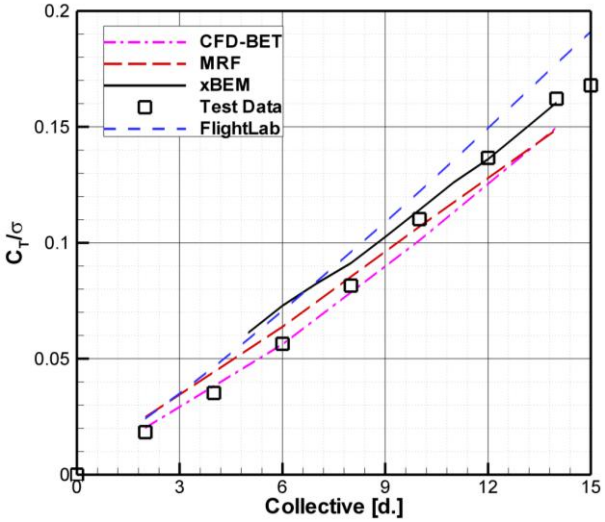

Figure 10 Comparison of predictions with tested thrust generation for designed rotor at hover

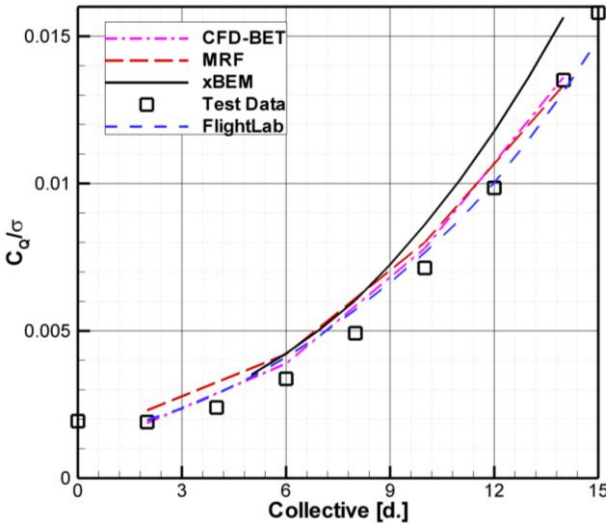

Figure 11 Comparison of predictions with tested power requirement of designed rotor at hover

The agreement between the predicted and measured hover performance is promising in terms of the analysis capability and manufacturing skills. Resulting power and thrust characteristics was sort of a blind test case for the engineers performed analysis and manufacturing. The discrepancy between computed and tested results is within acceptable range. Moreover the trend in the results with changing collective and rotational speed settings is consistent with the available data in literature. The tested rotor blade was the first blade which was totally designed and manufactured within the company using its own resources. Since it was the first rotor blade, aeromechanic design characteristics were defined with conventional choices. Achieving the predicted and expected performance at the tests of the initial rotor design, new rotors with more advanced and innovative concepts will be designed and manufactured in near future. The aerodynamic characterization of the manufactured conventional blade is also extended by flowfield measurements to examine the prediction capabilities of the analysis tools and to investigate rotary wing specific aeromechanic phenomena more closely.

4.2 Wake Measurements

The primary aim of the aeromechanic measurements applied during whirl tower tests was to validate the hover performance of the designed and manufactured rotor in terms of thrust generation and power requirement before it is installed to the built UAV rotorcraft platform for ground and flight tests. As shown in previous subchapters the primary aim is complied with satisfactory accuracy. As secondary aim the testing capability on whirl tower is planned to be extended for collecting flowfield data from the wake of the rotor. In the design phase of the rotor, extensive CFD analyses were applied to capture and characterize the wake structure behind the rotor for varying rotor blade pitch settings. Test capability which enables measurement of unsteady velocity components and identification of the position of the tip vortices will be a valuable asset for validation of the design tools and investigation of flow physics underlying the advanced rotor blade concepts.

The TWT, operates in open environment hence the test section is exposed to environmental effects. The hover tests are constrained to the conditions in which the wind speed does not exceed 3 knots. Since management of light exposure and particle seeding in the open environment is complicated and inefficient, optical based velocity measurement techniques such as LDV and PIV is considered to be inapplicable for the whirl tower system at least in near future. Hotwire method is also eliminated because of possible ruggedness problem due to the possibility of existence of free particles in open environment.

Utilization of fast response multi-hole probes is selected as proper candidate for the velocity measurement technique from the whirl tower tests. In recent years with the emergence of miniaturized pressure transducers, and advances in MEMS technology, high bandwidth pressure transducers and transducer arrays that are favorable for fast-response rates, enabled new multi-hole probes designs [13]. Probe designs with a tip diameter of 1-2 mm, which composes the embedded transducers, are currently available in the market thanks to the miniature size of these transducer arrays. In the whirl tower tests fast response 5 Hole probes produced by Aeroprobe is utilized. The probes have straight tips and provide velocity

data with response rate upto 4kHz. Figure 12 presents the photograph of the probe used in the tests.

Figure 12 Fast response 5 hole probe manufactured by Aeroprobe Company

5 fast response five-hole probes are arranged in rake configuration for the initial velocity measurement tests. The probes are separated from each other by one tenth of rotor radius distance. The rake is fixed in the downwash below the rotor at z/R = 0.25 location. Measurements are applied for varying collective settings of the rotor. The applied fast response five-hole probe configuration in the test is depicted in Figure 13. In near future, probes will be traversed in the flowfield and the wake of the hovering rotor will be characterized.

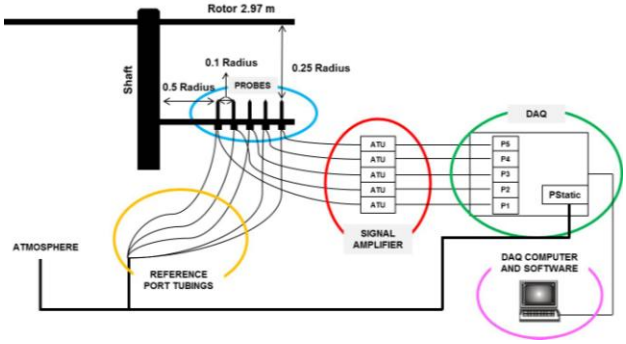

Figure 13 Probe configuration utilized in the initial velocity measurement tests from the downwash.

The time series pressure data measured by fast response probes are reduced to velocity components by using the Multiprobe software supplied by Aeroprobe. The sample data collected through tests and resulting axial downwash velocity component after reduction is depicted in Figure 14. Investigating the initial measurements it was observed that the fast response probes exhibited promising performance on capturing the crucial unsteady flow features in hovering rotor wake.

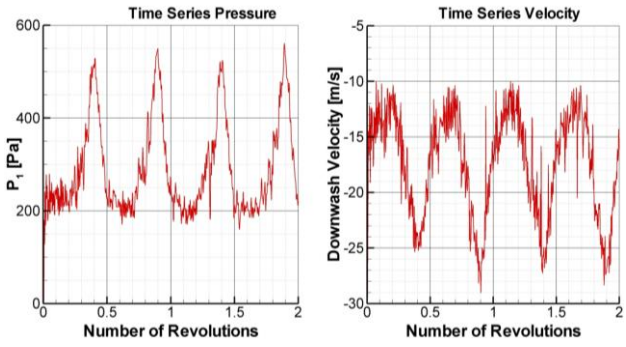

Figure 14 Sample time series data collected from fast response multihole probes

The time series downwash velocity components obtained from measurements are reduced to variation of velocity through one rotor revolution by ensemble averaging. Figure 15 presents the comparison of the predicted radial variation of the circumferentially averaged axial downwash velocity component with the measured data for 10 degrees of collective setting. The velocity magnitude in the graph is normalized with the maximum downwash velocity measured throughout tests. This initial comparison shows promising agreement between test and analysis results although improvements on both methods are ongoing and the studies related to measurement technique are not finalized.

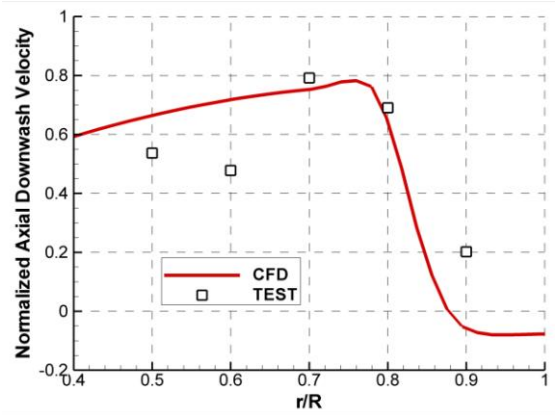

Figure 15 Radial variation of circumferentially averaged axial downwash velocity at z/R = 0.25

The reduced data from probe located in the middle of the rake at r/R= 0.7 position is compared with CFD results in Figure 16 for 10 degrees of collective setting case. The y axis of the figure is normalized with the maximum downwash velocity measured throughout tests. Although there seems to be a small bias error between the results of the two methods, trend of velocity variation through one revolution is captured to a certain extent. The studies focusing on improvement of data reduction technique and new provision design for fixture of the probe in the flowfield are expected to enhance the agreement between the results. Achieving satisfying correlation between test data and analysis results, further tests will be utilized by traversing the probes in the downwash of the rotor.

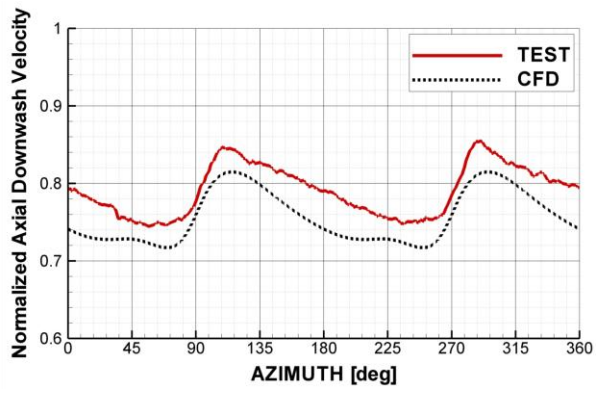

Figure 16 Variation of downwash velocity throughout one revolution below rotor at z/R = 0.25, r/R=0.7

Besides quantifying the wake characteristics with velocity measurements by 5 hole probes the qualitative

measurements will also be applied by means of visualization of the rotor downwash by entraining smoke in the flow field. Water based persistent smoke generated from the smoke generator machine is ducted to different nozzle positions located above and side of the rotor disk plane. The inflow generated by the hovering rotor sucks the injected smoke to the flow field and makes the contraction of the inflow visible with vortical wake. The variation of the path of smoke through the downwash is captured by the high speed cameras. In the initial phase, visualized flowfield with smoke is used to assess the variation of tip vortices and size of their cores by changing collective setting qualitatively. In the following step, captured images with high speed cameras will be post processed to evaluate the axial convection and radial contraction of the tip vorticies through the wake and evaluated results will be compared with the measurements collected by traversed fast response 5 hole probes.

4.3 Acoustic Measurements

Noise signature of the manufactured prototype is characterized with the measurements obtained by microphones located at different positions around the test facility. Microphones manufactured by PCB Piezotronics are used throughout the tests. Noise data is acquired with National Instrument data acquisition system with sampling rate of 20 kHz over two minutes. Figure 17 depicts the microphone layout near the test setup. Two microphones are placed at 2 radius distance away from the rotor axis at 1m height and different azimuth positions in order to investigate non-symmetrical effects of the whirl tower if exists. Third microphone is placed at 3 radius distance with 1m height and the last one is placed at the same distance with 2m height.

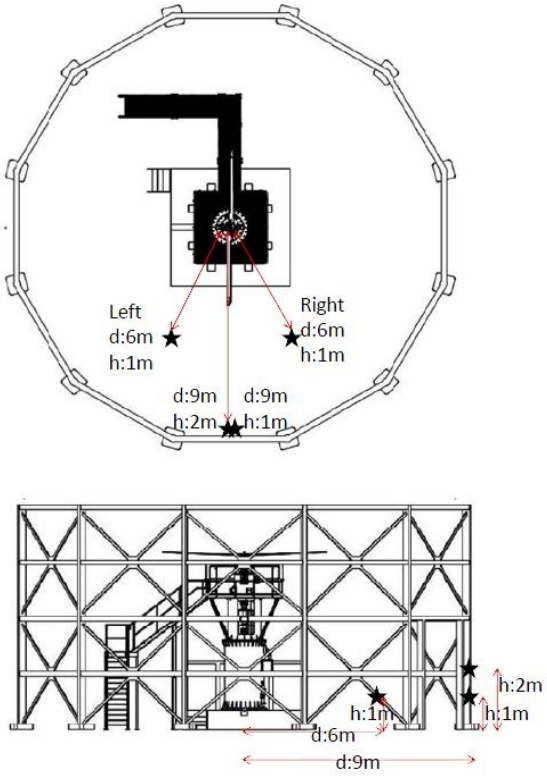

Figure 17 Layout of microphones in test field

Acoustic measurements are performed at 540 RPM rotational speed for collective settings varying from 0 to 14 degrees. In Figure 18, measured sound pressure level of the rotor is compared with the calculations performed with empirical relation available in literature developed by whirl tower tests [14]. In the same figure the result obtained from solution of FW-H equation by CFD solver using the blade surface as noise source is also presented. The measurements and predictions show similar trends. The sound pressure level measured from whirl tower tests is compared with the available data in literature for varying thrust coefficient values in Figure 19. Measured noise level correlates well with the previously published data that is evaluated from similar whirl tower tests[15].

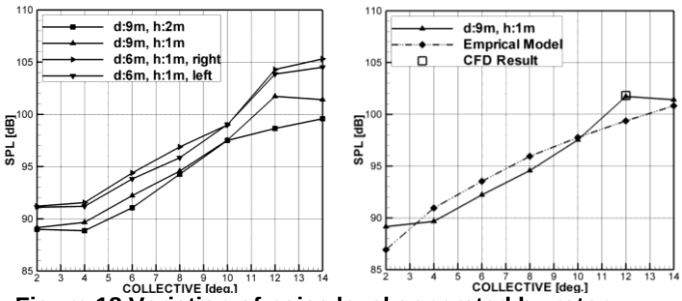

Figure 18 Variation of noise level generated by rotor by changing collective setting

The measurements with varying microphone positions are still under investigation and comparison with analytical/numerical results will be extended with the conclusion of the ongoing analyses. Noise measurement tests for hover and flyover maneuvers will be conducted with the built unmanned rotorcraft prototype following the whirl tower tests. The noise measurement and prediction capability gained throughout the analysis and tests of the designed and built prototype will be improved further and the gained skills will be utilized for evaluation of aerocoustics characteristics of advanced rotor concepts in the near future.

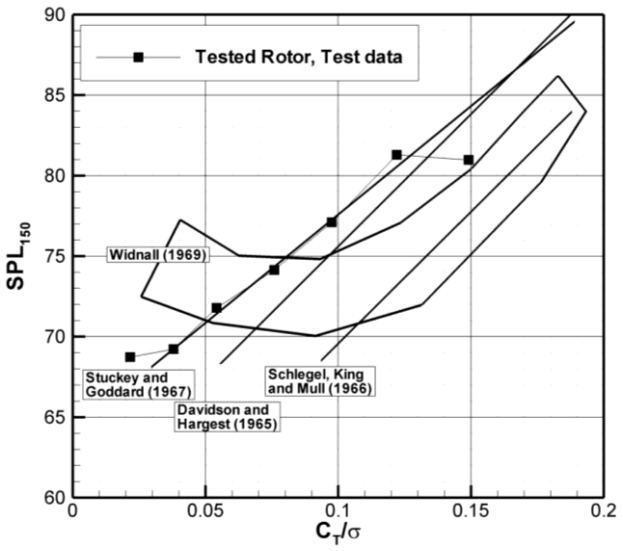

Figure 19 Comparison of noise measurements from whirl tower with literature data

5 CONCLUSIONS

The RANS and BEM theory based aerodynamic analysis tools are validated for hovering rotor performance prediction. The validated tools are utilized to design a 3 meter radius rotor that will be installed on an unmanned rotorcraft. The designed rotor is manufactured as a prototype and tested on the in-house whirl tower test facility. The instrumented test system is utilized to perform the aerodynamic measurements for validation of the proposed performance of the designed rotor.

The asset attained from both measurements and analyses will be employed in future studies to examine innovative concepts on rotor designs and validation of new design concepts.

6 ACKNOWLEDGMENTS

This study was supported by TUBITAK project No:3110496, Rotor and Whirl Tower Development Project

The authors present special thanks to Ufuk Başlamışlı for his valuable contributions to the test data reduction

7 REFERENCES

[1] F.,K.,Straub et al., “Development and Whirl Tower Test of the SMART Active Flap Rotor”, Symposium on Smart Structures and Materaials, San Diego, CA, March 14-18, 2004.

[2] Lorber, P., O’Neil, J., Hein, B., Isabella, B.,Andrews, J., Brigley, M., Wong, J., LeMasurier, P. and Wake, B., “Whirl and Wind Tunnel Testing of the Sikorsky Active Flap Demonstration Rotor,” American Helicopter Society 67th Annual National Forum, Virginia Beach, VA, May 3-5, 2011.

[3] Hasegawa, Y. et al (2001), Experimental and Analytical Results of a Whirl Tower Test of ATIC Full Scale Rotor System, American Helicopter Society 57th Annual Forum, Washington, May 2001.

[4] J. Chorin. "Numerical solution of Navier-stokes equations". Mathematics of Computation. 22. 745–762.1968.

[5] M. Rhie and W. L. Chow. "Numerical Study of the Turbulent Flow Past an Airfoil with Trailing Edge Separation". AIAA Journal. 21(11). 1525–1532. November 1983.

[6] Van Leer. "Toward the Ultimate Conservative Difference Scheme. IV. A Second Order Sequel to Godunov’s Method". Journal of Computational Physics. 32. 101–136. 1979.

[7] Caradonna, F.X. and Tung, C., “Experimental and Analytical Studies of a Model Helicopter Rotor in Hover,” NASA Technical Memorandum 81232, 1981

[8] O.J. Boelens, H. van der Ven, B. Oskam, and A.A. Hassan. “The boundary conforming discontinuous Galerkin Finite Element Approach for Rotorcraft Simulations,” J. of Aircraft, 39(5):776-785, 2002.

[9] Steijl, R., G. Barakos, and K. Badcock. "A framework for CFD Analysis of Helicopter Rotors in Hover and Forward Flight." International journal for numerical methods in fluids 51.8 (2006): 819-847.

[10] Hariharan, Nathan, et al. "Tip Vortex Field Resolution Using an Adaptive Dual-Mesh Computational Paradigm." 49th AIAA Aerospace Sciences Meeting including the New Horizons Forum and Aerospace Exposition, AIAA 2011. Vol. 1108. 2011

[11] Peterson, Randall L., and William Warmbrodt. "Hover Test of a Full-scale Hingeless Helicopter Rotor: Aeroelastic Stability, Performance and Loads Data." NTIS, SPRINGFIELD, VA(USA), 1984, 52 (1984).

[12] Peterson, Randalll. "Full-scale hingeless rotor performance and loads.", NASA Technical Memorandum 110356, 1995.

[13] D. Telionis, Y. Yang, “Recent Developments in Multi-Hole Probe (MHP) Technology”, 20th International Congress of Mechanical Engineering, November 15-20, 2009, Gramado, RS, Brazil

[14] Johnson, Wayne. Helicopter theory. Courier Dover Publications, 2012

[15] Stuckey, T. J., and J. O. Goddard. "Investigation and Prediction of Helicopter Rotor Noise Part I. Wessex Whirl Tower Results." *Journal of Sound and Vibration* 5.1 (1967): 50-80